Molecular Biology of the Cell
Vol. 15, 4512–4521, October 2004

The Fusome Mediates Intercellular Endoplasmic Reticulum Connectivity in *Drosophila* Ovarian Cysts

Erik L. Snapp, Takako Iida, David Frescas, Jennifer Lippincott-Schwartz, and Mary A. Lilly*

Cell Biology and Metabolism Branch, National Institute of Child Health and Human Development, National Institutes of Health, Bethesda, MD 20892

Submitted June 11, 2004; Revised July 22, 2004; Accepted July 23, 2004
Monitoring Editor: Allan Spradling

***Drosophila* ovarian cysts arise through a series of four synchronous incomplete mitotic divisions. After each round of mitosis, a membranous organelle, the fusome, grows along the cleavage furrow and the remnants of the mitotic spindle to connect all cystocytes in a cyst. The fusome is essential for the pattern and synchrony of the mitotic cyst divisions as well as oocyte differentiation. Using live cell imaging, greenfluorescent protein–tagged proteins, and photobleaching techniques, we demonstrate that fusomal endomembranes are part of a single continuous endoplasmic reticulum (ER) that is shared by all cystocytes in dividing ovarian cysts. Membrane and lumenal proteins of the common ER freely and rapidly diffuse between cystocytes. The fusomal ER mediates intercellular ER connectivity by linking the cytoplasmic ER membranes of all cystocytes within a cyst. Before entry into meiosis and onset of oocyte differentiation (between region 1 and region 2A), ER continuity between cystocytes is lost. Furthermore, analyses of *hts* and *Dhc64c* mutants indicate that intercellular ER continuity within dividing ovarian cysts requires the fusome cytoskeletal component and suggest a possible role for the common ER in synchronizing mitotic cyst divisions.**

INTRODUCTION

Gametogenesis takes place within germline cysts in a wide array of organisms (Telfer, 1975; Büning, 1994; de Cuevas *et al.*, 1997). In *Drosophila* a single oocyte develops within the environment of a 16-cell cyst. The development of this cyst occurs in a series of morphologically defined regions (see Figure 1A). Cyst production begins when a germline stem cell divides asymmetrically to produce a cystoblast. The cystoblast undergoes four synchronous mitotic divisions (regions 1 and 2a), with incomplete cytokinesis, to produce a cluster of 16 cells that are connected via arrested mitotic cleavage furrows (reviewed in de Cuevas *et al.*, 1997). Later in oogenesis, the arrested cleavage furrows mature into stable ring canals and are reinforced with an actin cytoskeleton (reviewed in Mahajan-Miklos and Cooley, 1994). Initially, all 16 cystocytes develop in synchrony. However, as development proceeds, differentiation within the cyst becomes asynchronous. Ultimately, only one cell commits to meiosis and differentiates as the oocyte, whereas the other 15 cystocytes enter the endocycle and develop as trophic nurse cells.

A unique membranous organelle, the fusome, grows and branches along the spindle equators after each mitotic division to physically connect all cells within a cyst. The fusome is found in the germline cysts of *Drosophila* as well as other insects (reviewed in Telfer, 1975; McKearin, 1997). The *Drosophila* fusome is comprised of cytoplasmic endomembranes, membrane skeletal proteins and polarized microtubules (reviewed in de Cuevas *et al.*, 1997; McKearin, 1997).

Molecular genetic studies over the last ten years indicate the fusome mediates several essential steps in germline cyst development (reviewed in McKearin, 1997). The differentiation of the oocyte depends on the production of a polarized network of microtubules within the cyst, that facilitates the directional transport of specific mRNAs and proteins from the pronurse cells to the single cell that will become the oocyte (Koch and Spitzer, 1983; Theurkauf *et al.*, 1992, 1993). The fusome organizes the network microtubules within developing ovarian cysts and is required for the microtubule-dependent restriction of oocyte markers (Grieder *et al.*, 2000). In addition, the fusome directs the pattern of cystocyte interconnections by anchoring one pole of each mitotic spindle, thus orienting the plane of cell division (Telfer, 1975; Storto and King, 1989; Lin and Spradling, 1995).

Mutations in genes that encode the cytoskeletal component of the fusome including *α-spectrin* and *β-spectrin*, and the adducin-like protein *hts*, result in a reduced number of cyst divisions and a block in oocyte differentiation (Lin *et al.*, 1994; de Cuevas *et al.*, 1996; de Cuevas and Spradling, 1998). In the absence of the fusome, cysts develop with random patterns of interconnections and no signs of polarity. However, it is unclear if the fusome plays an instructive role in the differentiation of the oocyte through participation in specific signaling pathways or if its sole function in oocyte differentiation is to facilitate the organization of microtubules into a polarized network. Thus, the fusome provides a useful model to examine how developmentally directed modifications of an intracellular organelle might function to facilitate differentiation.

Article published online ahead of print. Mol. Biol. Cell 10.1091/mbc.E04–06–0475. Article and publication date are available at www.molbiolcell.org/cgi/doi/10.1091/mbc.E04–06–0475.

* Corresponding author. E-mail address: mlilly@helix.nih.gov.

Abbreviations used: ER, endoplasmic reticulum; FRAP, fluorescence recovery after photobleaching; FLIP, fluorescence loss in photobleaching; D_{eff}, effective diffusion coefficient; M_f, mobile fraction; ROI, region of interest.

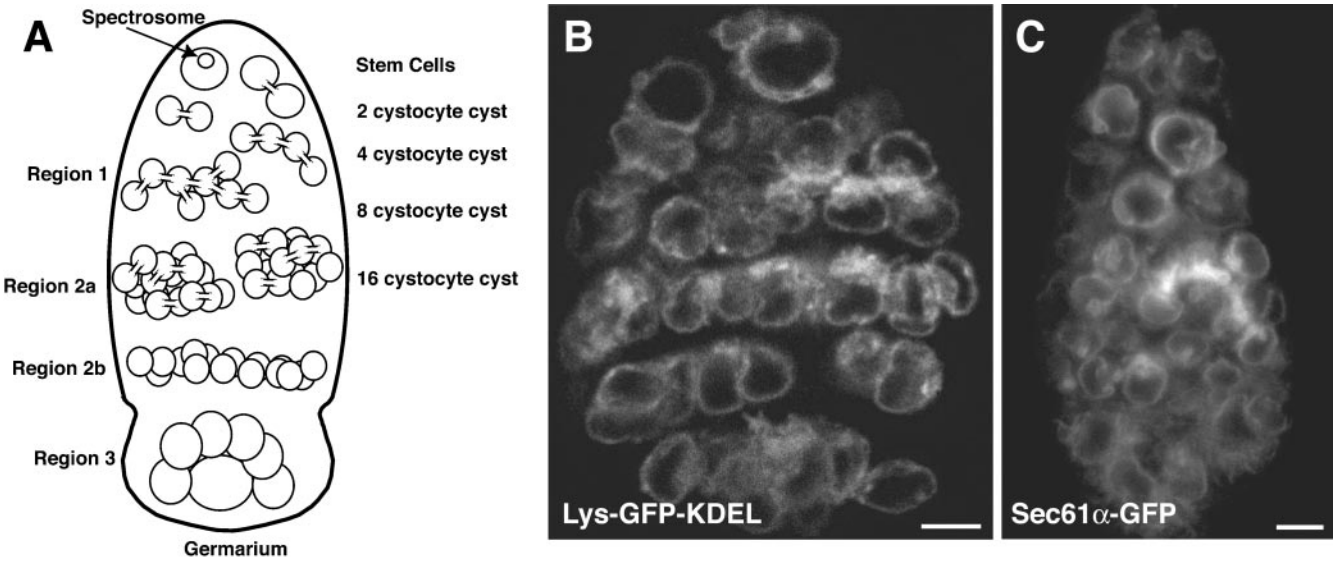

Figure 1. Visualization of ER GFP proteins in live germaria. (A) Diagram of a germarium from a *Drosophila* ovary. The four mitotic cyst divisions take place in region 1 of the germarium. In region 2a, all 16 cells (referred to as cystocytes) enter premeiotic S phase. In region 2b, a meiotic gradient forms with the two cystocytes with four ring canals progressing to pachytene. As cysts enter region 3 of the germarium (stage 1) only the cell that is destined to become the oocyte remains in the meiotic cycle. In contrast, the 15 mitotic sisters of the oocyte enter the S phase of the first endocycle on their way to becoming highly polyploid nurse cells. (B) Expression and distribution of Lys-GFP-KDEL in a live germarium. (C) Expression and distribution of Sec61α-GFP in a live germarium.

Although progress has been made toward revealing the molecular composition of the proteinaceous components of the fusome, the origin and nature of the membranous component remains poorly understood. Based on electron microscopy studies, the ribosome deficient endomembranes of the fusome have been described as vesicles or an interconnected network of tubules that resemble modified endoplasmic reticulum (ER) or Golgi (Koch and King, 1966; Mahowald, 1971; Lin *et al.*, 1994; McKearin and Ohlstein, 1995). Consistent with this observation, León and McKearin (1999) reported the enrichment on *Drosophila* fusome structures of the cytoplasmic protein TER94, which associates with both the Golgi complex and the ER in vertebrates (Uchiyama *et al.*, 2002). In this study, we have used live imaging and photobleaching of green fluorescent protein (GFP)-tagged proteins to gain insight into the membranous component of the *Drosophila* fusome.

MATERIALS AND METHODS

Drosophila Stocks

The *hts*^{1} allele (Yue and Spradling, 1992) was a gift from Allan Spradling. *Dhc64*$^{3-2}$ and *Dhc64*$^{6-12}$ (McGrail and Hays, 1997) were from Margaret de Cuevas. The *P{w+ Pvas-gfp}* flies were a gift from Akira Nakamura (Nakamura *et al.*, 2001). The Sec61α-GFP line (ZCL0488 from the Flytrap collection) was generously provided by Lynn Cooley. Sec61α is a 10-membrane–spanning resident ER protein that associates in a heterotrimer with Sec61β and γ to form the core of the ER protein translocation channel, the translocon (Johnson and van Waes, 1999).

Transgenic lines were generated in a *w*^{1118} background using standard techniques (Spradling, 1986). Two independent insertions of P{w^{+}, UASp::Lys-GFP-KDEL} and two independent insertions of P{w^{+}, UASp: galactosyltransferase-GFP} into the second and third chromosomes were obtained. The nanos-Gal4:VP16 driver (Van Doren *et al.*, 1998) was used to express UASp-transgenes in the germline. Transgenic flies of the following genotypes were used in this article: *w*^{1118}*; P{w*$^{+}$*, UASp::Lys-GFP-KDEL}; P{w*$^{+}$*, nanos-Gal4:VP16}; w*^{1118}*; P{w*$^{+}$*, UASp::galactosyltransferase-GFP}; P{w*$^{+}$*, nanos-Gal4:VP16}; w*^{1118}*; hts*^{1}*/hts*^{1}*; P{w*$^{+}$*, UASp::Lys-GFP-KDEL}/P{w*$^{+}$*, nanos-Gal4: VP16}; w*^{1118}*; P{w*$^{+}$*, UASp::Lys-GFP-KDEL}/+; Dhc64*$^{3-2}$*/Dhc64*$^{6-12}$*, P{w*$^{+}$*, nanos-Gal4:VP16}. Dhc64*$^{6-12}$*, P{w*$^{+}$*, nanos-Gal4:VP16}, w*^{1118}*; P{w*$^{+}$ *Pvas-GFP}; hts*^{1}*/hts*^{1} chromosomes were generated by meiotic recombination. All additional stocks were obtained from the Bloomington Stock Center.

Plasmid Constructions

To visualize the ER, a marker protein, lysozyme-GFP-KDEL (Lys-GFP-KDEL), was expressed in the germline using the *Drosophila* Gal4-UAS system. Lysozyme-GFP-KDEL was constructed by fusing the complete coding sequence of hen's egg lysozyme with a COOH-terminal enhanced GFP (BD Biosciences, Clontech, Palo Alto, CA) followed by a KDEL ER retention signal (Munro and Pelham, 1987). The Golgi apparatus marker protein, galactosyltransferase (GalTase-GFP) has been previously described (Cole *et al.*, 1996). Separate DNA fragments encoding Lys-GFP-KDEL or GalTase-GFP were cloned into pUASp (Rorth, 1998) to generate a p[w^{+}, UASp-lysozyme-GFP-KDEL] or a p[w^{+}, UASp-galactosyltransferase-GFP] transgene. Lys-GFP-KDEL and GalTase-GFP expressing flies produced viable adults.

Immunofluorescence and Imaging of Live and Fixed Ovaries

Ovaries were dissected, immunostained, and mounted as described previously (Lin *et al.*, 1994). Antibodies were used at the following concentrations: rabbit anti-α-spectrin (Byers *et al.*, 1987; Dubreuil *et al.*, 1987) at 1:100, mouse anti-α-spectrin 3A9 (Dubreuil *et al.*, 1987) at 1:5 (Developmental Studies Hybridoma Bank, University of Iowa), mouse anti-Hts (Zaccai and Lipshitz, 1996) at 1:5, rabbit anti-GFP (Molecular Probes, Eugene, OR) at 1:800 and mouse anti-GFP (Molecular Probes; JL-8) at 1:1000. Secondary antibodies conjugated to Alexa 594 or Alexa 488 (Molecular Probes) were used at 1:800 dilution.

Live ovaries were placed flat on poly-lysine–coated Lab-Tek chambered coverglasses from Nalge Nunc (Naperville, IL). Chambers were then filled with *Drosophila* Ringer's solution (Tübingen and Düsseldorf). Confocal microscope images of live and fixed ovaries were captured on a LSM 510 confocal microscope (Zeiss, Thornwood, NY) using a 488-nm line of a 40-mW Ar/Kr laser with a 505–530 emission filter for GFP and a 543 nm HeNe laser line with a 560–615 emission filter. Images were captured with a 1.2 NA 63× water objective and a 1.3 NA plan-neo 40× oil objective. Image analysis was performed using NIH Image 1.62 and Zeiss LSM image examiner software. Composite figures were prepared using Photoshop 7.0 and Illustrator 9.0 software (Adobe, San Jose, CA).

Photobleaching and Analysis

Fluorescence recovery after photobleaching (FRAP) and fluorescence loss in photobleaching (FLIP) were performed by photobleaching a small region of interest (ROI) and monitoring fluorescence recovery or loss over time, as

described previously (Siggia *et al.*, 2000; Snapp *et al.*, 2003). Fluorescence intensity plots and D_{eff} measurements were calculated as described previously (Siggia *et al.*, 2000; Snapp *et al.*, 2003). To create the fluorescence recovery curves, the fluorescence intensities were transformed into a 0–100% scale and were plotted using Kaleidagraph 3.5 (Synergy Software, Reading, PA). For Figure 3, the postbleach asymptote intensity of the ROI was designated as 100%. For Figure 4–6, the prebleach intensity of the ROI was designated as 100%. p values were calculated using a Student's two-tailed *t* test in Excel (Microsoft, Redmond, WA).

RESULTS

The Fusome Contains Continuous ER Membranes

Initially, we considered the possibility that the fusome membranes are derived from the Golgi apparatus or the ER. This was suggested by the observation that *Drosophila* fusome structures are enriched with the cytoplasmic protein TER94, which associates with both the Golgi complex and the ER in vertebrates (Leon and McKearin, 1999; Uchiyama *et al.*, 2002). To characterize the structure and origin of the membranous component of the fusome, we expressed the lumenal ER-marker protein, Lys-GFP-KDEL, the resident ER membrane protein, Sec61α-GFP, or the Golgi marker, GalTase-GFP (Cole *et al.*, 1996), in ovarian cysts. In confocal micrographs of live germaria, Lys-GFP-KDEL and Sec61α-GFP both labeled amorphous tubular elements that extend from the nuclear envelope throughout the cytoplasm (Figure 1, B and C), consistent with an ER distribution. Interestingly, the fluorescence of both proteins was more intense in thick branching structures between adjacent cystocytes. To determine whether these accumulations of ER membranes correspond to fusomes, we performed immunofluorescence with antibodies against the fusomal components α-Spectrin and Hts. We observed extensive colocalization of Lys-GFP-KDEL and Sec61α-GFP with the fusomal markers (Figure 2, A–D). In contrast, GalTase-GFP localized to discrete punctate structures throughout the cytoplasm of all cystocytes. The puncta did not colocalize with the fusome marker Hts (Figure 2E). This pattern is similar to the distribution of the Golgi marker anti-α-mannosidase 2 previously described by Cox and Spradling (2003). Additional membranes of other origins may be present within the fusome. Nonetheless, our data support the conclusion that fusomes are significantly enriched in ER membranes and that these probably represent the primary source of fusome membranes.

In stem cells, spectrin accumulates in a structure termed the spectrosome (Lin *et al.*, 1994). It has been proposed that the spectrosome is the precursor of the fusome and may serve as a source of cytoskeletal proteins and membranes (Lin *et al.*, 1994). In Figure 2, A and C, the ER colocalizes with spectrosomes. However, the ER is less enriched than in the fusome structures for either Lys-GFP-KDEL or Sec61α-GFP, similar to previous observations (Lin *et al.*, 1994).

Ovarian Cysts Share a Common ER

Whether the fusome membranes consist of discrete ER-derived vesicles or form a network of interconnected tubules has remained unresolved with evidence for both types of fusome membrane structures observed by electron microscopy (Telfer, 1975; Büning, 1994; Lin *et al.*, 1994; McKearin, 1997). It is worth noting that the ER of animal cells is an ideal example of an interconnected membranous compartment and typically exists as a continuous network of branching tubules connected to the nuclear envelope. However, the fusomal membranes may not be continuous with the cytoplasmic ER of the cystocytes.

We exploited photobleaching methods to directly assess the membrane continuity of fusomal membranes (Ellenberg

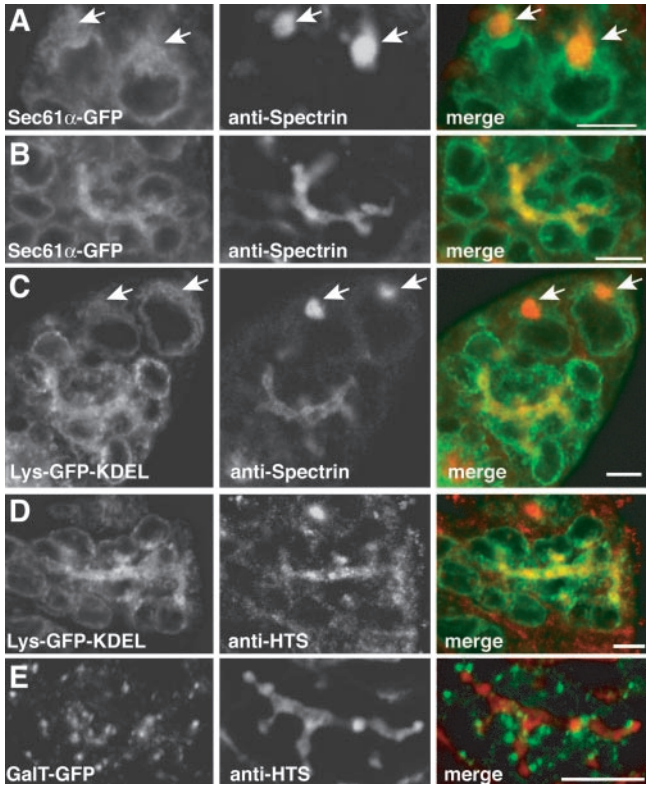

Figure 2. Fusomal membranes arise from the ER. (A–D) Germaria expressing the ER markers Sec61α-GFP (A and B) or Lys-GFP-KDEL (C and D) were fixed and labeled with the fusome markers anti-spectrin (A–C) or anti-Hts (D and E). Regions of colocalization in the merged images (yellow) appear within the ER accumulations between cystocytes, but not within the cystocyte cytoplasm to reveal the ER origin of fusome membranes. In A and C, large Spectrin accumulations (spectrosomes) in stem cells are indicated by white arrows. These structures do contain ER-labeling, though the structures are not substantially enriched with ER accumulations. (E) A cyst from a GalTase-GFP ovary stained with anti-Hts. No significant colocalization between these markers was observed. Bars, 5 μm.

et al., 1997; Lippincott-Schwartz *et al.*, 2001). First, we confirmed the suitability of Lys-GFP-KDEL and Sec61α-GFP (unpublished data) as highly mobile diffusing molecular markers by performing Fluorescence Recovery after Photobleaching (FRAP) of Lys-GFP-KDEL expressed in cystocytes from region 1 of the germarium (unpublished data) and stem cells (Figure 3A). For example, a small ROI in a stem cell expressing Lys-GFP-KDEL was photobleached with a high intensity laser beam, destroying the GFP fluorescence. Recovery of fluorescence into the photobleached ROI indicated that unbleached Lys-GFP-KDEL molecules outside of the photobleached ROI had diffused into the photobleached ROI, whereas photobleached molecules had diffused out of the ROI. The fluorescence recovery was rapid and did not involve gross structural changes of the ER membranes, consistent with the diffusion of a highly mobile protein. The diffusion coefficient (D_{eff}) within the cystocytes (D_{eff} = 0.84 ± 0.4 μm²/s, Mobile fraction ~ 100%, n = 5) represents a value consistent with diffusion of a protein within the crowded lumen of the ER (Dayel *et al.*, 1999). Sec61α-GFP also diffuses readily. However, as expected, the membrane protein diffuses more slowly through the more viscous environment of the membrane (D_{eff} = 0.2 ± 0.02 μm²/s, Mobile fraction ~ 100%, n = 2). Thus, both proteins freely

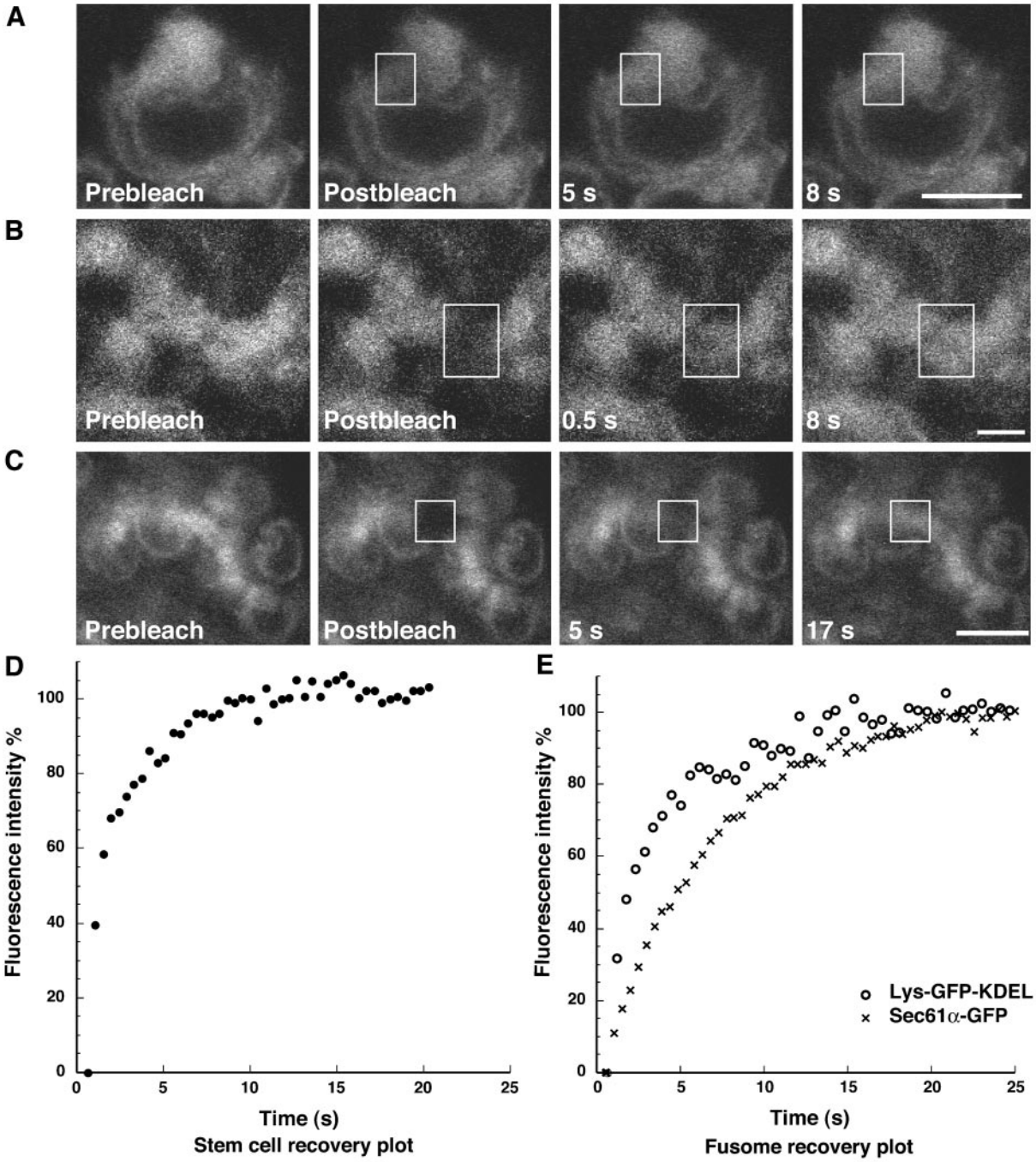

Figure 3. Membrane and lumenal ER markers exhibit distinct diffusion properties in the fusome. (A and D) A small ROI (white outlined box) within a stem cell was briefly photobleached and the rapid fluorescence recovery was monitored visually and quantitatively. Bar, 5 μm. (B and E) Mobility of Lys-GFP-KDEL within fusomes is similarly rapid, as revealed by the FRAP experiment within the fusome. Bar, 1 μm. (C and E) Diffusion of Sec61α-GFP within fusomes is slower than the lumenal ER marker Lys-GFP-KDEL. Bar, 5 μm.

diffuse within the ER and therefore represent suitable markers to examine membrane continuity.

To determine whether fusome membranes were vesicular or formed a continuous network, we compared the D_{eff} of Lys-GFP-KDEL and Sec61α-GFP within the fusome ER-derived membranes. The organization of the membranes should affect the apparent mobility of the lumenal and membrane proteins. If the fusome were composed of discrete vesicles, then movement of both proteins would depend on the movement of molecular motors or diffusion of the whole vesicles. Both proteins would be predicted to move with identical dynamics. In contrast, if the proteins reside within continuous tubules, then the distinct environments of the ER lumen and the more viscous ER membrane would dominate protein mobility. The two proteins would be predicted to diffuse at different rates.

FRAP of the fusome membranes revealed that Lys-GFP-KDEL fluorescence recovers rapidly within the fusome (D_{eff}

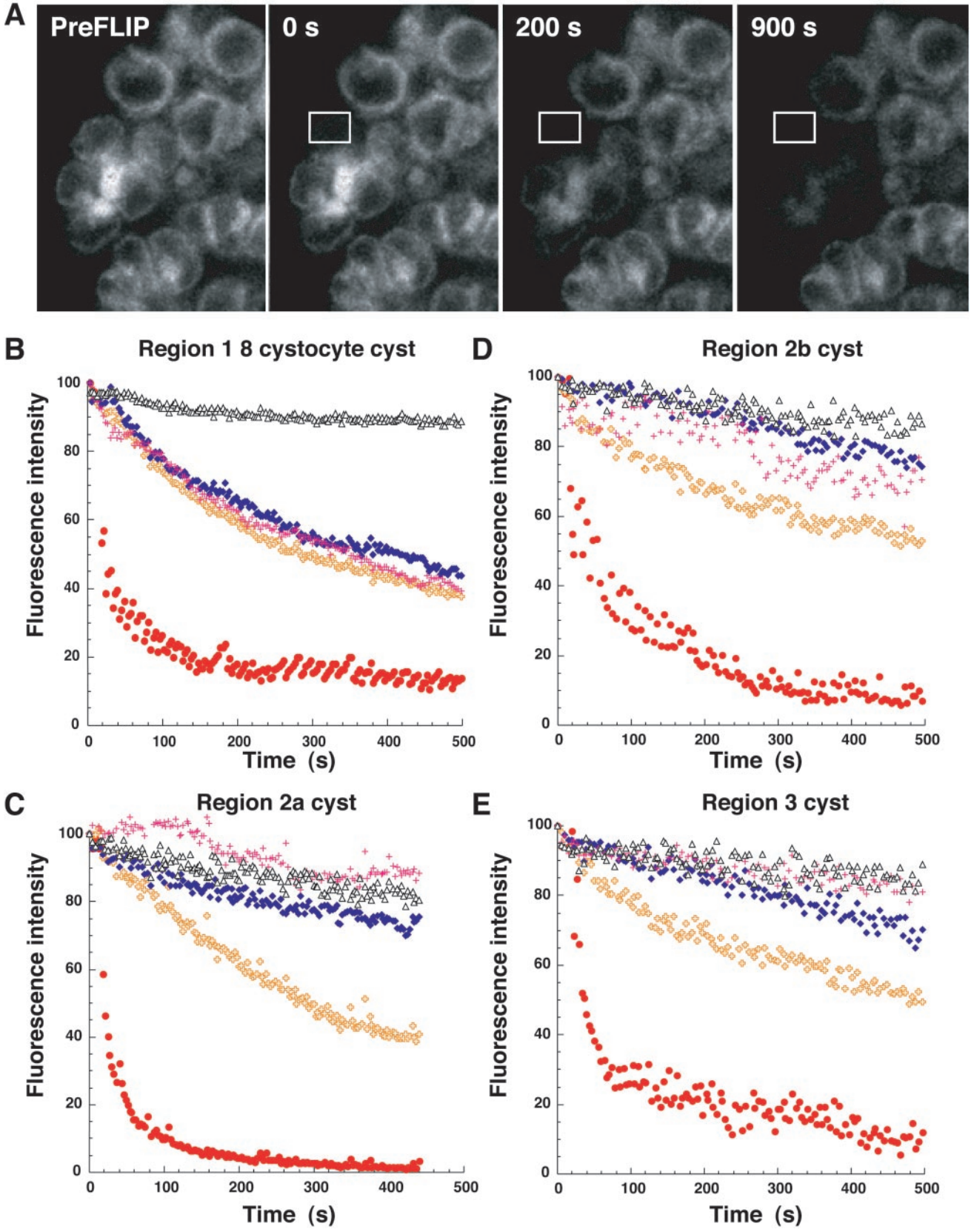

Figure 4. FLIP analysis of ER continuity in cysts from regions 1–3 of the germarium. (A) Repetitive photobleaching of cystocytes within a region 1 eight-cell cyst, in a small ROI (white outline box), was performed. The 0s image represents the first image after the first photobleach. The same ROI was photobleached every seven seconds. By 900 s, nearly all fluorescence had been depleted from all of the cystocytes within a cyst, whereas adjacent cystocyte fluorescence was unaffected. Bar, 5 μm. (B–E) Rates of loss of fluorescence for individual cystocytes are

= 1.5 ± 0.4) $\mu m^2/s$, n = 3; Figure 3, B and E), whereas Sec61α-GFP recovers significantly more slowly (p = 0.0002; D_{eff} = 0.15 ± 0.03 $\mu m^2/s$, n = 5). The D_{eff} values for each protein are not statistically significantly different for each protein in cystocytes (p = 0.062 for Lys-GFP-KDEL and 0.094 for Sec61α-GFP). In both cases, recovery occurred on both sides of the photobleached ROI, consistent with diffusion, a nondirectional process. Thus, the FRAP results are most consistent with the organization of the fusome as a continuous network of membranes, similar to cytoplasmic ER.

The FRAP results raised an important question. Are the ER-derived fusome membranes continuous with the cytoplasmic ER of cells within the cyst? While FRAP can be used to infer compartment continuity, a second photobleaching method, Fluorescence Loss in Photobleaching (FLIP; Ellenberg *et al.*, 1997), can be used to directly probe membrane continuity of an entire structure by repeatedly photobleaching a discrete ROI (Lippincott-Schwartz *et al.*, 2001). If all of the fluorescent molecules are mobile and can diffuse through the ROI in a short period, all of the fluorescence within a compartment will be depleted. We performed FLIP on cysts with 2, 4, or 8 cells in region 1. Data for a representative 8 cell cyst are shown in Figure 4, A and B. Surprisingly, when we bleached a small ROI of the cytoplasmic ER from an individual cystocyte, within a cyst, we observed a rapid depletion of fluorescence from the entire fusome, as well as the cytoplasmic ER in all cystocytes throughout the cyst (Figure 4A). Similar results were obtained if the photobleach ROI was placed within the fusome (unpublished data). In all FLIP experiments, fluorescence in other cysts within the same germarium was not significantly depleted, confirming that fluorescence loss in cells within the cyst of interest was not caused by photobleaching due to the imaging conditions. These dramatic results reveal that not only are the ER membranes within the fusome continuous, but more remarkably, the ER of all cystocytes are interconnected to form a common ER.

Cyst ER Connectivity Is Developmentally Regulated

Next, we investigated the maintenance of the common ER during oogenesis. The structure of the cytoskeletal component of the fusome changes after the completion of the final mitotic cyst division (region 2a, see Figure 1a). Staining with antibodies against Hts and α-Spectrin reveals a decrease in the thickness of the fusome beginning in region 2a cysts. This change in fusome structure correlates with the time that cell cycle synchrony is lost as cystocytes asynchronously progress through premeiotic S phase (Lin *et al.*, 1994). By region 2b, the cytoskeletal component of the fusome begins to deteriorate and by region 3, characteristic fusome structures are no longer visible (Lin *et al.*, 1994; de Cuevas *et al.*, 1996).

We asked whether the ER of cells within an ovarian cyst remain interconnected after the completion of the mitotic cyst divisions, as the nurse cells and oocyte begin to pursue their unique developmental and cell cycle programs. To address this question, we used FLIP to compare the continuity of the ER within cysts before (region 1) and after the final mitotic division (region 2a). Figure 4, B and C, graphically reveal an abrupt change in ER connectivity within cysts between region 1 and region 2a. In contrast to the rapid fluorescence loss within the 8 cystocyte region 1 cyst in Figure 4B, the rate of fluorescence loss in cystocytes within region 2a cyst decreases dramatically (Figure 4C). The fluorescence intensities of the directly photobleached cystocytes (red circles) decrease rapidly and exponentially. However, while the cystocyte closest to the cystocyte being photobleached does lose fluorescence, the loss is at a much slower linear rate. In addition, the fluorescence loss from other cystocytes within the same cyst now resembles the minimal loss of fluorescence of cystocytes in adjacent cysts (black triangles). Similar results were observed for FLIP experiments of regions 2b and 3 cysts (Figure 4, D and E). The abrupt change from a steep exponential drop in fluorescence in adjacent cystocytes, to a shallow linear decrease in fluorescence between cysts in regions 1 and 2a, argues for a substantial loss of cyst ER connectivity after the completion of the mitotic cyst divisions. This result is surprising, in that Lys-GFP-KDEL does not noticeably redistribute and continues to colocalize with the cytoskeletal component of the fusome in region 2a (unpublished data). The change in ER connectivity at the mitotic/meiotic boundary represents a newly defined step in cyst development.

ER Connectivity Correlates with Mitotic Synchrony

The temporal coincidence of the loss of ER connectivity and the onset of cell cycle asynchrony suggest a potential role for the shared ER in region 1 cysts; the ER may be important for synchronizing the mitotic cyst divisions. To explore this possibility, we examined ER connectivity in female sterile mutants of *hu-li-tai-shao* (*hts*) and the Dynein subunit, *Dhc64c*. In hts^1 cysts, no fusome structures can be detected by immunofluorescence or by electron microscopy (Lin *et al.*, 1994). Conversely, cysts from $Dhc64c^{3-2}/Dhc64c^{6-12}$ transheterozygous females retain fusome structures, but these structures frequently are fragmented and do not extend into all cells of the cyst (McGrail and Hays, 1997). Both hts^1 and $Dhc64c^{3-2}/Dhc64c^{6-12}$ dramatically reduce the number of cyst divisions leading to the production of egg chambers that contain fewer than 16 cells. However, the mutants have very different effects on mitotic synchrony. hts^1 cysts undergo asynchronous divisions as evidenced by the presence of egg chambers that contain cyst cell numbers that do not conform to multiples of 2^n (i.e., 2, 4, 8, 16; Yue and Spradling, 1992). In contrast, 95% of $Dhc64c^{3-2}/Dhc64c^{6-12}$ egg chambers contain a 2^n number of germline cells, indicating mitotic synchrony is maintained (McGrail and Hays, 1997). We reexamined both the hts^1 and $Dhc64c^{3-2}/Dhc64c^{6-12}$ mutant phenotypes and determined that mitotic divisions involving four or more cells (4–8 and 8–16) require a synchronizing regulatory mechanism that is disrupted in hts^1 but not in $Dhc64c^{3-2}/Dhc64c^{6-12}$ mutants (unpublished data).

Given the differences in the ability of *hts* and *Dhc64c* mutants to support mitotic synchrony during cyst divisions, we then asked whether the two mutants differ in ER con-

Figure 4 (facing page). plotted and compared for cysts in different regions. For each plot, the red circles indicate the fluorescence of the cystocyte containing the photobleach ROI. Orange +'s, blue diamonds, and pink +'s indicate the fluorescence intensities of other cystocytes within the same cyst. Orange +'s represent the cystocyte closest to the photobleached cyst and blue diamonds, and pink +'s represent the next closest cystocytes, respectively. The flat horizontal pattern of black triangles at the top of the plot represents the fluorescence intensity of an adjacent unconnected cyst and indicates that photobleaching is specific for the cystocytes within the cyst of interest. (B) In a representative region 1 eight-cell cyst, fluorescence loss in the photobleached cystocyte and adjacent cystocytes occurs in an exponential manner. (C–E) After the cysts have undergone the final round of mitosis, the FLIP experiments reveal a different pattern of fluorescence loss. The directly photobleached cystocytes (red circles) of region 2a, 2b, and 3 cysts also lose fluorescence exponentially. In contrast, adjacent cystocytes, within the same cyst, slowly lose fluorescence in a shallow linear manner.

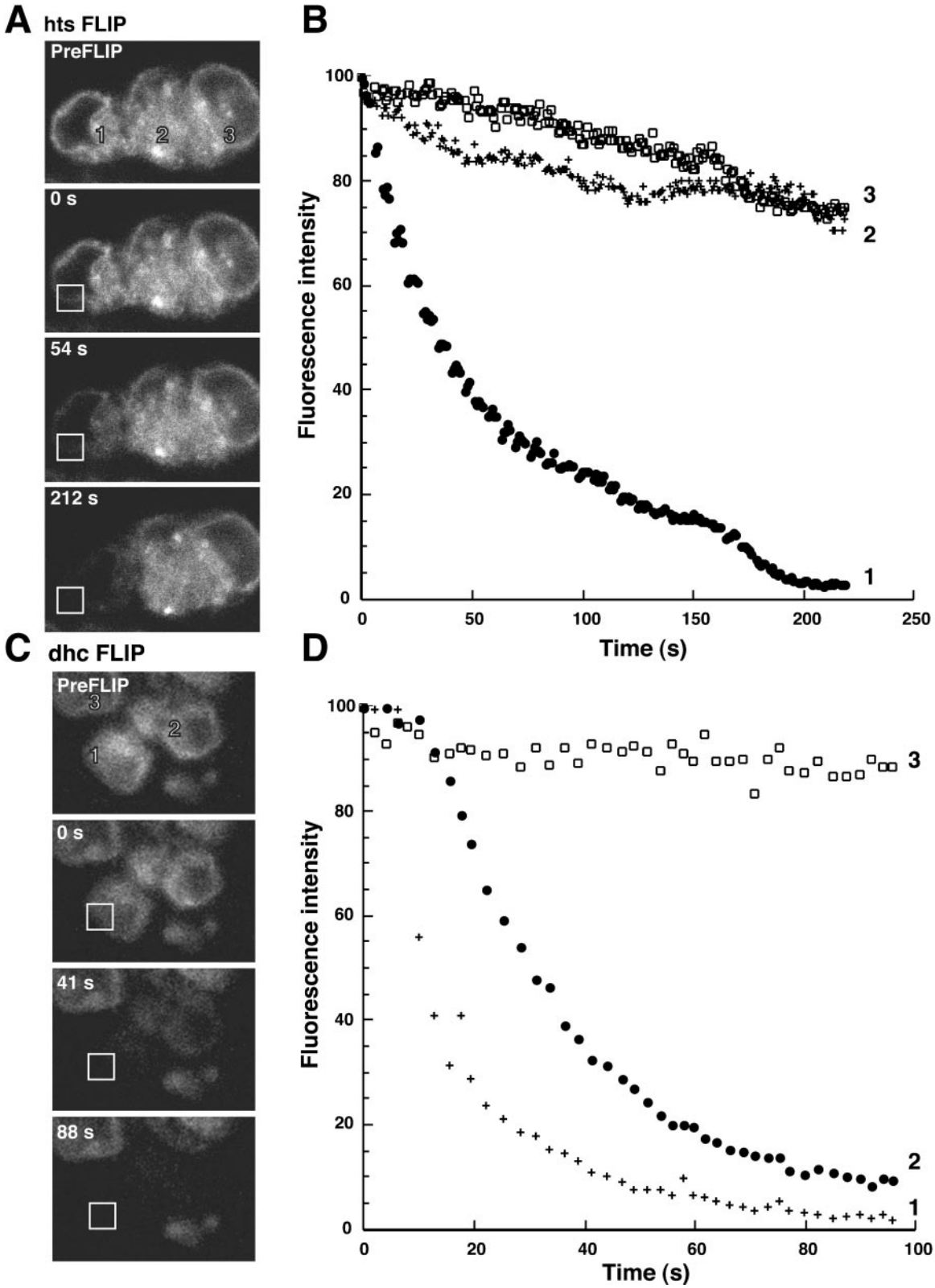

Figure 5. ER continuity in *hts* and *Dhc64* mutant germaria. (A) FLIP of *hts*^{1} mutant germarium. The cystocyte on the far left (1) was repeatedly photobleached over time. Adjacent cystocyte (2 and 3) fluorescence was also monitored and the fluorescence intensities were plotted in B. Only the photobleached cystocyte (1; ●) loses fluorescence exponentially, whereas adjacent cystocytes (2 and 3; □ and +'s) lose minimal fluorescence. Compare with Figure 4, A and B. (C and D) FLIP of *Dhc64* mutant ovarian cyst, as in A and B. Note that cystocyte 3 is in an adjacent cyst and should not be connected to the photobleached cystocyte. Cystocyte 3 (□) does not lose any fluorescence during the time course of the experiment. However, both the photobleached cystocyte (1, ●) and the adjacent cystocyte (2, +) undergo a rapid exponential loss of fluorescence, consistent with ER continuity. Bars, 5 μm.

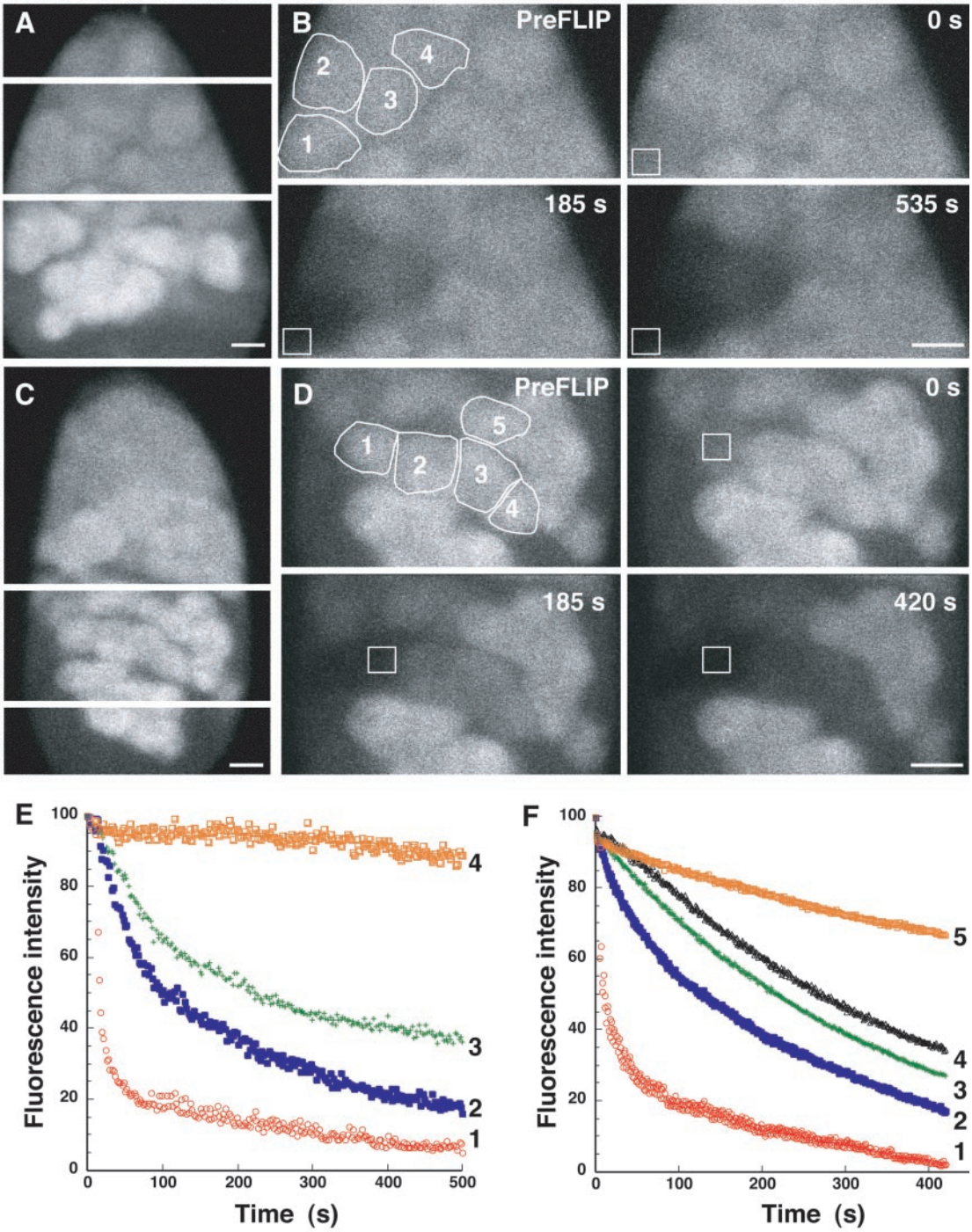

Figure 6. Cytoplasmic continuity in wild-type and *hts*^{1} cysts. FLIP was performed on (A) wild-type and (C) *hts*^{1} cysts expressing cytoplasmic Vasa-GFP. (A) Representative germarium from an ovary of a cytoplasmic GFP expressing fly. (B) FLIP of a wild-type outlined cystocyte (1) within the region between the two white bars in A. Fluorescence loss throughout a cyst (cells 1, 2, and 3) is observed, whereas adjacent cysts (i.e., cell 4) do not lose fluorescence. Thus, cells 1–3 are part of a connected cyst and share a common cytoplasm. (C) Representative germarium from a cytoplasmic GFP expressing *hts*^{1} ovary. (D) FLIP of *hts*^{1} cells, within the region between the two white bars in C, reveal that cells 1–4 are part of the same cyst and share a common cytoplasm. (E and F) Similar results and evidence of cytoplasmic connectivity were observed for cysts in different regions of the germaria of both wt and *hts*^{1} flies. The exponential fluorescence loss within the cysts in B and D is represented quantitatively for the photobleached cystocytes: 1, red circles; 2, blue squares; 3, green +'s, 4, black triangles (for D), and an unconnected cystocyte-orange squares (4 for B and 5 for D). Bars, 5 μm.

nectivity. We probed the degree of ER continuity between cystocytes in the two mutants by FLIP (Figure 5). Repetitive photobleaching of individual cystocytes of *hts*^{1} mutants failed to deplete fluorescence in adjacent cystocytes in the same cyst (Figure 5, A and B). In contrast, FLIP of *Dhc64c*$^{3-2}$/*Dhc64c*$^{6-12}$ mutant cystocytes rapidly depleted fluores-

cence of all cystocytes within the same cyst (Figure 5, C and D). Thus, the mitotically synchronous $Dhc64c^{3-2}/Dhc64c^{6-12}$ cysts maintain an interconnected ER, whereas hts^{1} cysts do not. These data are consistent with EM studies that indicate that the membrane component of the fusome is absent in hts^{1} mutant germaria (Lin *et al.*, 1994). As a control, we determined that cytoplasmic connectivity is unaffected in hts^{1} mutants (Figure 6). Specifically, we found that a cytoplasmic GFP marker can freely diffuse between the cytoplasms of interconnected cystocytes in both wild-type and mutant cysts (Figure 6). These data confirm that cytoplasmic connectivity is insufficient to coordinate mitotic synchrony between cystocytes and support the model that the fusome is required to promote cell cycle synchrony. Our results raise the intriguing possibility that the membranous ER component of the fusome coordinates cell cycle synchrony during the mitotic cyst divisions.

DISCUSSION

We have found that the fusomal membranes represent a developmental modification of the ER, from an intracellular organelle, to an organelle with the potential to foster intercellular communication. This work has lead to three important conclusions: 1) The fusomal membranes are derived from the ER; 2) The fusome membranes are continuous with the cytoplasmic ER; and 3) All the cells within a single ovarian cyst share a common ER. We found that the common ER connectivity is developmentally regulated and dramatically dissipates before the onset of cell cycle asynchrony within the cyst. Finally, our characterization of hts^{1} and *Dhc64* mutants indicates that ER connectivity correlates with the retention of cell-cycle synchrony during the germline cyst divisions.

How might a common ER contribute to cyst development during early oogenesis? One potential functional role for the fusomal membranes was first suggested by the observation that mutations in *bam* and *bgcn*, two genes that control the developmental switch from stem cell to cystoblast, alter the membranous composition of the spectrosome (McKearin and Ohlstein, 1995), the likely precursor of the fusome (Lin *et al.*, 1994). Another possibility is that the common ER may promote mitotic synchrony in cystocytes that are not directly connected. Mitotic synchrony is essential for the production of the invariant pattern of interconnections found in *Drosophila* ovarian cysts. Mitotic effectors such as cyclin A (CycA) have been shown to transiently associate with the fusome during G2 and prophase (Lilly *et al.*, 2000). At least one signal must exist upstream of CycA to coordinate the activity of CycA and other mitotic effectors. Modulation of calcium levels is an attractive potential signaling candidate. Calcium signaling plays several roles in mitotic pathways (Berridge, 1995) and the ER is the primary site of calcium storage and release in eukaryotic cells (Baumann and Walz, 2001). Another possible mechanism by which the fusome ER may regulate the cell cycle is suggested by the findings that the SCF component Cul-1, as well as polyubiquitinated cyclin E, localize to the fusome (Ohlmeyer and Schupbach, 2003). Cul-1 has been implicated in the regulated destruction of a wide array of proteins involved in both cell cycle regulation and signal transduction (reviewed in Deshaies, 1999). Interestingly, the membrane-associated protein TER94/VSC/p97, which localizes to the fusome (Leon and McKearin, 1999), has also been implicated in ubiquitin-dependent degradation in mammals (Dai and Li, 2001). Thus, the ER component of the fusome may provide a surface for regulated protein degradation. An additional possibility is that the common ER may serve as a transport system that regulates trafficking of signal containing transmembrane and membrane-associated proteins between cystocytes in a manner analogous to the ER of plasmodesmata in plants (Zambryski, 2004). It will be important in future studies to distinguish between the roles of the cytoskeletal proteins and the ER in fusome function.

Our results have implications for communication in other syncitial systems as well, such as spermatozoa in mammals (Fawcett *et al.*, 1959; Rasmussen, 1973; Clermont and Rambourg, 1978) and the ectoderm of hydra cnidoblasts. In both of these examples, groups of synchronously developing cells contain evidence of intercellular ER connections between dynamic ring canals (Fawcett *et al.*, 1959). Thus, a shared ER may be general mechanism for coordinated cyst development.

ACKNOWLEDGMENTS

We thank Margaret de Cuevas, Lynn Cooley, Allan Spradling, Akira Nakamura, and the Bloomington stock center for fly stocks and Margaret de Cuevas for critical reading of the manuscript. T.I. is a Japan Society for the Promotion of Science Research Fellow in Biomedical and Behavioral Research at the National Institutes of Health. E.L.S. was supported by a Pharmacology Research and Training fellowship.

REFERENCES

Baumann, O., and Walz, B. (2001). Endoplasmic reticulum in animal cells and its organization into structural and functional domains. Intern. Rev. Cytol. *205*, 149–215.

Berridge, M. (1995). Calcium signaling and cell proliferation. Bioessays *17*, 491–500.

Büning, J. (1994). The Insect Ovary: Ultrastructure, Previtellogenic Growth and Evolution, New York: Chapman & Hall.

Byers, T.J., Dubreuil, R., Branton, D., Kiehart, D.P., and Goldstein, L.S.B. (1987). *Drosophila* spectrin. II. Conserved features of the alpha-subunit are revealed by analysis of cDNA clones and fusion proteins. *105*, 2103–2110.

Clermont, Y., and Rambourg, A. (1978). Evolution of the endoplasmic reticulum during rat spermiogenesis. Am. J. Anat. *151*, 191–212.

Cole, N.B., Smith, C.L., Sciaky, N., Terasaki, M., Edidin, M., and Lippincott-Schwartz, J. (1996). Diffusional mobility of Golgi proteins in membranes of living cells. Science *273*, 797–801.

Cox, R.T., and Spradling, A.C. (2003). A Balbiani body and the fusome mediate mitochondrial inheritance during *Drosophila* oogenesis. Development *130*, 1579–1590.

Dai, R.M., and Li, C.H. (2001). Valosin-containing protein is a multiubiquitin chain targeting factor required in ubiquitin-proteasome degradation. Nat. Cell Biol. *3*, 740–744.

Dayel, M.J., Hom, E.F.Y., and Verkman, A.S. (1999). Diffusion of green fluorescent protein in the aqueous-phase lumen of endoplasmic reticulum. Biophys. J. *76*, 2843–2851.

de Cuevas, M., Lee, J.K., and Spradling, A.C. (1996). α-spectrin is required for germline cell division and differentiation in the *Drosophila* ovary. Development *122*, 3959–3968.

de Cuevas, M., Lilly, M.A., and Spradling, A.C. (1997). Germline cyst formation in *Drosophila*. Annu. Rev. Genet. *31*, 405–428.

de Cuevas, M., and Spradling, A.C. (1998). Morphogenesis of the *Drosophila* fusome and its implications for oocyte specification. Development *125*, 2781–2789.

Deshaies, R.J. (1999). SCF and Cullin/Ring H2-based ubiquitin ligases. Annu. Rev. Cell Dev. Biol. *15*, 435–467.

Dubreuil, R.R., Byers, T.J., Branton, D., Goldstein, L.S.B., and Kiehart, D.P. (1987). *Drosophila* spectrin. I. Characterization of the purified protein. *105*, 2095–2102.

Ellenberg, J., Siggia, E.D., Moreira, J.E., Smith, C.L., Presley, J.F., Worman, H.J., and Lippincott-Schwartz, J. (1997). Nuclear membrane dynamics and reassembly in living cells: targeting of an inner nuclear membrane protein in interphase and mitosis. J. Cell Biol. *138*, 1193–1206.

Fawcett, D.W., Ito, S., and Slautterback, D. (1959). The occurrence of intercellular bridges in groups of cell exhibiting synchronous differentiation. J. Biophys. Biochem. Cytol. *5*, 543–560.

Grieder, N.C., de Cuevas, M., and Spradling, A.C. (2000). The fusome organizes the microtubule network during oocyte differentiation in *Drosophila*. Development *127*, 4253–4264.

Johnson, A.E., and van Waes, M.A. (1999). The translocon: a dynamic gateway at the ER membrane. Annu. Rev. Cell Biol. *7*, 90–95.

Koch, E.A., and King, R.C. (1966). The origin and early differentiation of the egg chamber of *Drosophila melanogaster*. J. Morph. *119*, 283–304.

Koch, E.A., and Spitzer, R.H. (1983). Multiple effects of colchicine on oogenesis in *Drosophila*: induced sterility and switch of potential oocyte to nurse-cell developmental pathway. Cell Tissue Res. *228*, 21–32.

Leon, A., and McKearin, D. (1999). Identification of TER94, an AAA ATPase protein, as a Bam-dependent component of the *Drosophila* fusome. Mol. Biol. Cell *10*, 3825–3834.

Lilly, M.A., de Cuevas, M., and Spradling, A.C. (2000). Cyclin A associates with the fusome during germline cyst formation in the *Drosophila* ovary. Dev. Biol. *218*, 53–63.

Lin, H., and Spradling, A.C. (1995). Fusome asymmetry and oocyte determination in *Drosophila*. Dev. Genet. *16*, 6–12.

Lin, H., Yue, L., and Spradling, A.C. (1994). The *Drosophila* fusome, a germline-specific organelle, contains membrane skeletal proteins and functions in cyst formation. Development *120*, 947–956.

Lippincott-Schwartz, J., Snapp, E., and Kenworthy, A. (2001). Studying protein dynamics in living cells. Nat. Rev. Mol. Cell Biol. *2*, 444–456.

Mahajan-Miklos, S., and Cooley, L. (1994). Intercellular cytoplasm transport during *Drosophila* oogenesis. Dev. Biol. *165*, 336–351.

Mahowald, A.P. (1971). Formation of ring canals by cell furrows in *Drosophila*. Z. Zellforsch. mikrosk. Anat. *118*, 162–167.

McGrail, M., and Hays, T.S. (1997). The microtubule motor cytoplasmic dynein is required for spindle orientation during germline cell divisions and oocyte differentiation in *Drosophila*. Development *124*, 2409–2419.

McKearin, D. (1997). The *Drosophila* fusome, organelle biogenesis and germ cell differentiation: if you build it. Bioessays *19*, 147–152.

McKearin, D., and Ohlstein, B. (1995). A role for the Bag-of-marbles protein in the differentiation of cystoblasts from germline stem cells. Development *121*, 2937–2947.

Munro, S., and Pelham, H.R. (1987). A C-terminal signal prevents secretion of luminal ER proteins. Cell *48*, 899–907.

Nakamura, A., Amikura, R., Hanyu, K., and Kobayashi, S. (2001). Me31B silences translation of oocyte-localizing RNAs through the formation of cytoplasmic RNP complex during *Drosophila* oogenesis. Development *128*, 3233–3242.

Ohlmeyer, J.T., and Schupbach, T. (2003). Encore facilitates SCF-Ubiquitin-proteasome-dependent proteolysis during *Drosophila* oogenesis. Development *130*, 6339–6349.

Rasmussen, S.W. (1973). Ultrastructural studies of spermatogenesis in *Drosophila melanogaster*. Meigen. Z. Zellforsch. mikrosk. Anat. *140*, 125–144.

Rorth, P. (1998). Gal4 in the *Drosophila* female germline. Mech. Dev. *78*, 113–118.

Siggia, E.D., Lippincott-Schwartz, J., and Bekiranov, S. (2000). Diffusion in a inhomogeneous media: theory and simulations applied to a whole cell photobleach recovery. Biophys. J. *79*, 1761–1770.

Snapp, E., Altan, N., and Lippincott-Schwartz, J. (2003). Measuring protein mobility by photobleaching GFP-chimeras in living cells. In: Current Protocols in Cell Biology, eds. J. Bonifacino, M. Dasso, J. Harford, J. Lippincott-Schwartz, and K. Yamada, New York: John Wiley & Sons.

Spradling, A. (1986). P element-mediated transformation. In: *Drosophila*: A Practical Approach, ed. D. Roberts, Oxford: IRL Press, 175–199.

Storto, P.D., and King, R.C. (1989). The role of polyfusomes in generating branched chains of cystocytes during *Drosophila* oogenesis. Dev. Genet. *10*, 70–86.

Telfer, W.H. (1975). Development and physiology of the oocyte-nurse cell syncytium. Adv. Insect Physiol. *11*, 223–319.

Theurkauf, W.E., Alberts, B.M., Jan, Y.N., and Jongens, T.A. (1993). A central role for microtubules in the differentiation of *Drosophila* oocytes. Development *118*, 1169–1180.

Theurkauf, W.E., Smiley, S., Wong, M.L., and Alberts, B.M. (1992). Reorganization of the cytoskeleton during Drosophila oogenesis: implications for axis specification and intercellular transport. Development *115*, 923–936.

Uchiyama, K. *et al*. (2002). VCIP135, a novel essential factor for p97/p47-mediated membrane fusion, is required for Golgi and ER assembly in vivo. J. Cell Biol. *159*, 855–866.

Van Doren, M., Williamson, A.L., and Lehmann, R. (1998). Regulation of zygotic gene expression in *Drosophila* primordial germ cells. Curr. Biol. *8*, 243–246.

Yue, L., and Spradling, A.C. (1992). hu-li-tai shao, a gene required for ring canal formation during *Drosophila* oogenesis, encodes a homolog of adducin. Genes Dev. *6*, 2443–2545.

Zaccai, M., and Lipshitz, H.D. (1996). Differential distributions of two adducin-like protein isoforms in the *Drosophila* ovary and early embryo. Zygote *4*, 159–166.

Zambryski, P. (2004). Cell-to-cell transport of proteins and fluorescent tracers via plasmodesmata during plant development. J. Cell Biol. *164*, 165–168.